Development and Application of a Comprehensive Analysis of Liquid-Rocket Combustion

R. D. SUTTON,* W. S. HINES,* AND L. P. COMBS†
Rocketdyne/North American Rockwell, Canoga Park, Calif.

A comprehensive method for analyzing liquid-rocket engine combustion is introduced, which utilizes and unifies the results of analytical and experimental research in the fields of liquid-propellant injection and combustion. A system of 3-dimensional, time-dependent, nonlinear-conservation equations is derived and the necessary expressions for bipropellant spray-mass distribution, drop size, drop velocities, spray evaporation, and interphase drag are presented. Specialized application of the general model to the analysis of ablative-chamber compatibility is summarized and illustrated.

Nomenclature

A = area
a = local speed of sound
$a, b, C_1 \ldots C_6$ = empirical spray coefficients, Eq. (15)
C_D = drag coefficient
$C_{k'}$ = approximate evaporation rate coefficient
c = mixture ratio
c_p = specific heat at constant pressure
D = droplet diameter
$\mathscr{D}$ = molecular diffusivity
$\mathbf{F}$ = drag-force vector
F = component of drag force
g_c = gravitational coefficient
H = enthalpy $= \int_{T^o}^{T} \sum_i \omega_i c_{p_i}\, dt + \sum_i \omega_i H^o{}_{f_i}$
$H^o{}_{f_i}$ = heat of formation of species i at standard state
ΔH_v = heat of vaporization
k_g = thermal conductivity
k' = droplet-evaporation coefficient
M_w = molecular weight
m = droplet mass
$\dot{m}$ = rate of change of mass
N = droplet concentration (no./volume)
$\dot{N}$ = number flow rate of droplets
N_{EL} = number of injection elements
Nu = Nusselt number
p = pressure
Q = spray heating rate
$\mathbf{q}$ = heat-flux vector $= -k_g \operatorname{grad} T - \sum_i \rho \mathscr{D}_i H_i \operatorname{grad} \omega_i$
Re = Reynolds number
R_u = universal gas constant
r = radial coordinate, volumetric gas-phase reaction rate
T = temperature
t = time
$\mathbf{U}_i$ = ith species diffusion velocity
$\mathbf{u}$ = flow-velocity vector
u = component of flow velocity
W = propellant mass flux at a spatial mesh point
w = propellant mass flux contribution from an injection element to a mesh point
w_{001} = $w(x, y, z)$ for $x = y = 0, z = 1$
$\dot{w}$ = weight flow rate
x, y, z = rectangular coordinates (referenced to an injection element)
z = axial coordinate
Z_o = axial plane separating injection/atomization and rapid combustion zones
γ = ratio of specific heats
ρ = density
τ = stress tensor
θ = angular coordinate
$\Omega_{i,j}$ = proportional mass fraction of species i generated per unit weight of propellant j burned
ω_i = mass fraction of ith species in a gas mixture
ω = volumetric gas-generation rate
ϕ = velocity potential

Superscripts

$( )'$ = perturbation, deviation from mean value
$(\bar{\ })$ = average value
n = concerned with the nth initial droplet-size group
o = standard state

Subscripts

BU = breakup or disintegration of droplets
d = droplet
i = concerned with ith chemical species
j = concerned with jth propellant
l = liquid
o = initial, reference or stagnation value
s = stagnant, surface or stream-tube value
r, θ, z = in the coordinate direction
v = vapor or vaporization

Vector Operators

grad $( ) = \nabla( )$ = gradient of a scalar quantity
div $( ) = \nabla \cdot ( )$ = divergence of a vector quantity
$\mathbf{u;u}$ = dyadic product

Presented as Paper 70-622 at the AIAA 6th Propulsion Joint Specialist Conference, San Diego, Calif., June 15–19, 1970; submitted August 12, 1970; revision received September 23, 1971. The paper presents results of research conducted for the United States Air Force under Contracts AF49(638)-1705, sponsored by the Office of Scientific Research, Washington, D.C. and FO4611-68-C-0043, sponsored by the Air Force Rocket Propulsion Laboratory, Edwards, Calif.

Index categories: Propulsion, Combustion in Heterogeneous Media and Liquid Rocket Engines; Thermophysics and Thermochemistry, Thermal Modeling and Experimental Thermal Simulation.

* Member of Technical Staff.

† Member of Technical Staff. Member AIAA.

Introduction

DESIGN of liquid-rocket engines requires that efficient stable burning of the propellants, expansion of the combustion gases, and protection of the thrust-chamber walls be combined in a system of minimum weight. Historically, the analytical consideration of these separate requirements has been made in a rather uncoupled manner because of the complex nature of the over all problem. Similarly, analysis of the factors that influence the most complex aspect of the problem, the propellant combustion, has also involved use of a number of simplified models for individual processes. With the present availability of large high-speed digital computers, it appears possible to approach over all combustor design in an integrated fashion, and thereby, eliminate considerable development time and expense.

The state-of-the-art in analyzing liquid-rocket engine combustion is reviewed very briefly in this paper to indicate the need for a more comprehensive analytical formulation. Next, such a

formulation is presented in general vector-tensor form. It is structured to utilize, in a unified manner, available analytical and experimental technology, valid simplifications, initial and boundary conditions, and expressions for the interphase coupling terms. Finally, application of the comprehensive analysis in a series of computer programs for predicting effects of propellant combination, injector design variables, and chamber configuration on ablative-chamber wall compatibility is presented to illustrate potential design applications.

Previous Combustion Analyses

In this section, a background summarization is presented to reveal that the present analytical formulation utilizes, builds upon, and extends significantly the work of many previous investigators. Both steady-state and unstable combustion are included, but consideration is restricted to phenomena within the combustion chamber.

A majority of the analyses considered are based upon formulation and solution of a coupled system of differential and algebraic expressions representing the various physical and chemical processes that are involved in the conversion of propellants to combustion products. Realistic formulation requires that the controlling processes be identified and reasonably well understood. (To supplement the qualitative description sketched in the next few paragraphs, Refs. 1–3 may be consulted.)

Qualitative Understanding of Combustion Processes

Propellant combustion is usually recognized as being vaporization-rate limited and so is distributed spatially throughout the combustion chamber. For clarity and convenience in this discussion, and in the later model formulation, the combustor may be divided into a series of discrete zones as shown in Fig. 1 for a typical configuration. Certainly, transition from one zone to the next cannot be sharply defined, but is gradual. The positions and abruptness of these transitions are influenced by design variables, propellant combination and operating conditions. A few comments about each of these zones are pertinent before proceeding with the review.

Immediately adjacent to the propellant injector, the injection/atomization zone is least amenable to analytical description. With liquid injection concentrated at discrete sites, large gradients exist in all dimensions with respect to propellant mass fluxes and concentration, degree of atomization and spray dispersion, and properties of the gaseous medium. Spray droplets here are usually cold so the vaporization and burning rates are low. Gases in this zone are primarily either gaseous-injectants or recirculated combustion gases from the next zone downstream.

Completion of primary atomization and convective heating of spray droplets enhance vaporization rates, leading to comparatively high-chemical reaction rates in the rapid combustion zone. Upon burning, the volume of a liquid-propellant element is increased 100-fold or more. This expansion forces transverse flows from high-burning rate sites to low-burning rate sites as well as producing an axial acceleration. This provides some mixing but the sprays follow the gases only sluggishly, so spray-mass flux gradients are primarily degraded by injector-imposed geometric dispersion and interspray mixing. Lateral gas flows will be generated as long as appreciable spray-flux gradients persist, but eventually they become small compared with axial-flow velocities and the combustion field takes on a stream-tube flow appearance.

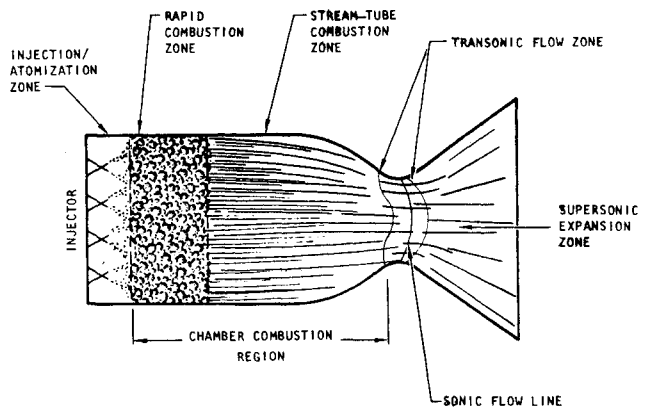

Fig. 1 Subdivision of combustion chamber into zones for analysis.

In the stream-tube combustion zone, the flow lacks the forced transverse convective components that are dominant in the earlier zones. Continued mixing depends upon turbulent exchange between neighboring, parallel-flowing striations, but flow velocities here are high, residence times are short, and turbulent mixing is not very effective. To a good approximation, mixing can be entirely neglected and the two-phase flow treated formally as stream tubes.

As sprays are accelerated and depleted, combustion rate per unit chamber length decays with increasing distance. Chemical reaction rates, on the other hand, remain high well into the exhaust nozzle. Then, as the combustion products expand through the nozzle, diminishing pressures and temperatures lower the gas-phase chemical reaction rates. Two-dimensional flow effects are also important in the transonic and supersonic flow zones. For most high-combustion efficiency rockets, spray combustion effects are negligible compared with gas dynamic effects in these downstream zones.

Steady-State Models

Nearly all previous combustion models for steady-state liquid-rocket operation share certain common features: they are based on one-dimensional flow equations; their central problem is burning of uniform, completely atomized propellant sprays; and they do not account analytically for lateral or circulating flows. In most analyses, spray vaporization was adopted as the rate-limiting process, a choice that was corroborated by the definitive work of Brokaw and Bittker.[4]

The earliest steady-state spray burning models were the most simplified; spray behavior was decoupled from the gas flow. Limiting case assumptions, e.g., no gas-droplet velocity lag, were used to get closed-form solutions, which were usually non-dimensionalized. Williams[5] reviewed this approach well. The generalized conclusions reached are now known to be inflexibly tied to the limiting-case assumptions.

Decoupled models were followed by analyses in which the spray and gas-phase equations were coupled but constant values were used for chamber pressure and combustion-gas properties, notably mixture ratio. As an example, Spalding[6] accounted for convective-spray particle-burning rates and drag but, to achieve a closed-form solution, identical fuel and oxidizer droplets all of one size were used. Priem and Heidmann[7] extended the analysis to a realistic spray droplet-size distribution, considered transient droplet-size distribution, considered transient droplet heating and turned to numerical, digital computer solutions. These developments were so important to useful applications of combustion analysis that their approach is sometimes the only work cited in reference to steady-state combustion models.

Following Priem's work, other investigations have refined his basic model and provided variable properties to remove some of its restrictions. The one-dimensional model in Ref. 2, for example, included axial pressure variation, secondary droplet breakup and separate fuel and oxidizer conservation equations, so that mixture ratio varied axially. Improved numerical integration schemes and two-flame front models of exothermic burning have been provided (e.g., Ref. 8). In most current models, an energy equation is avoided by assuming local stagnation reaction equilibrium and adiabatic "frozen" expansion to the flow conditions.

One-dimensional steady-state models are relatively easy to use. Chamber design, propellant property and combustion gas property data are necessary, but the most crucial input data are spray droplet-size distributions (which provide the only link to injector design) and the expressions used for the coupling terms.

However, purely one-dimensional models cannot show dependence nor provide information on essentially multidimensional problems, such as effects of lateral gradients in flow rates and mixture ratio, axially-distributed atomization, circulating flows, film-coolant flows, etc. These are largely injection/atomization and rapid combustion zone phenomena; it is inappropriate to apply a one-dimensional model where they are predominant,[2] although many users ignore this fact.

To rectify this deficiency, some quasi-multidimensional models have been formulated using multiple coupled one-dimensional flows to represent the injection/atomization zone for a single injection element (e.g., Ref. 2). Because injection element design details are intimately interwoven in the model, extensions to other designs are difficult and expensive. This approach is not widely utilized.

Instability Models

The full range of liquid-rocket combustion-instability analysis has recently been fully systematized and detailed in the forthcoming ICRPG reference book on instability.[3] Instabilities are classified according to their dominant time varying processes. Within the scope of this paper, only those involving combustion-chamber resonance are of interest. The central problem in analyzing chamber-resonance instabilities is obtaining solutions in one or more spatial dimension and time for a coupled system of nonlinear transient conservation equations with appropriate boundary conditions. Almost invariably, constant injection rates are assumed for the injection-end boundary condition, with no coupling to the feed system. The instabilities treated are then essentially acoustic resonances of the combustion space, with complications introduced by the existence of two phases, distributed combustion-energy release, accelerative through-flow of gases, and discharge of products from the nozzle. Formulations in one dimension and time represent longitudinal modes of instability. The transverse (tangential and radial) modes, which are of more importance in practice, require transient formulation in two or three spatial dimensions.

These instabilities are driven by properly phased spatial energy addition to the gaseous phase. The most influential energy addition often occurs in the injection/atomization region, which is no more amenable to transient than to steady-state solution. For this and other reasons, the earliest instability models used a nonphysical global treatment of combustion, i.e., the time lag concept introduced by von Kármán in 1941. This approach was well-developed for feed-system coupled and longitudinal instabilities[9] before the more physical, local spray combustion techniques were applied to instability analysis. Primarily under Professor Crocco's tutelage at Princeton University, a succession of investigations has evolved an ever more complicated succession of n–τ instability models, which were summarized in Ref. 10. Since their treatment of the combustion processes is nonphysical, they are not considered further here.

More physically based instability models were formulated after the dominant combustion mechanisms were discerned and quantitative expressions for spray-gas coupling terms were developed. Programed for digital-computer solution, this class of instability model typically: 1) starts with more or less complete sets of nonlinear-conservation equations, 2) accounts for interphase exchange of mass and energy by nonlinear-physical coupling expressions, 3) uses some form of spatial-initial conditions supplied by a steady-state combustion program, 4) provides for perturbation of steady combustion by a finite-amplitude pressure disturbance, and 5) marches in time to determine growth or decay of wave motion induced by that disturbance.

A longitudinal mode model[11] first included physical coupling terms, using the same steady-state expression for droplet heating, evaporation and drag which Priem[7] had used in his steady-state model. Initial conditions were supplied from a one-dimensional steady-state model which assumed constant fuel/oxidizer-vaporization rate ratio; no axial gradients in gas-mixture ratio (and therefore, temperature and molecular weight) or droplet number concentration were included in the nonsteady model.

Tangential-wave motion was formulated by Priem and Guentert[12] by considering a quasi-one-dimensional annular volume near the combustor's wall to have no radial gradients and constant axial gradients given by the steady-state solution. Among other simplifications, this model is similar to that of Ref. 11 in the use of steady-state coupling terms, constant gas-phase mixture ratio and constant drop-number concentration.

Further, the elemental volume is required to contain a constant mass of gas, i.e., an overpressure at one point must be offset by an underpressure elsewhere. Perhaps this accounts for predicted critical-disturbance amplitudes being lower than those found experimentally. However, the relative stabilities of various engines and stabilization resulting from design changes are predicted correctly. Priem's model has been extended recently to propellant burning at supercritical pressure.[8]

Full two-dimensional formulations, in both r, θ, t and z, θ, t coordinates, have been developed[13] which are rigorous and nearly complete. The latter, including both tangential and longitudinal motion, is potentially the most versatile and accurate model available. However, even though droplet-conservation equations are used, drop-number concentration and mixture-ratio equations are not.

These recurrent omissions in existing models must lead to reduced accuracy as oscillation amplitudes increase. Constant drop-number concentration leads to errors in the local gasification rates; constant mixture ratio leads to errors in predicted local pressure, the principal model parameter, because it is calculated from the state equation. The n–τ models are subject to the same limitations. Thus, the foregoing models are physically limited to weak waves, which do not disturb the assumed initial condition appreciably.

These limitations have been avoided partially in a new longitudinal-instability model by Agosta,[14] in which mixture-ratio variation is accounted for by use of a quasi-steady mixture-ratio equation and tables of properties. Good agreement was shown between experimental and predicted pressures.

Formulation of a Comprehensive Combustion Model‡

In this section, a model formulation is stated without showing the derivation. Written in general vector-tensor notation, its completeness both avoids the limitations encountered in previous models and permits identifying the errors introduced with those simplifying assumptions required for making practical numerical calculations. Using continuum mechanics for both gas and liquid spray phases, the model expresses the three-dimensional dynamics of a multicomponent reacting gas stream which undergoes simultaneous exchange of mass, momentum, and energy with contained liquid bipropellant sprays.

Assumptions used in the derivation are: 1) ideal gas law is a valid state equation, 2) effects of turbulence can be neglected,§ 3) dilute sprays occupy a negligible fraction of chamber volume, 4) each drop-size group represents a separate liquid phase and exchange terms between liquid phases are not included, 5) drag contributes only kinetic energy to the spray-energy equation, and 6) secondary "shear" breakup of droplets initially formed during primary atomization produces resultant droplets so small that they evaporate immediately upon formation.

The formulation is structured to incorporate analytical correlations for the interphase-coupling terms, which appear on the right-hand sides of certain equations (they can be identified

‡ The formulation stated in this section was derived under Air Force Contract AF49(638)-1705. This work is reported in detail in Ref. 23.

§ Time-averaged perturbations become meaningless during acoustic instabilities, when mean-flow oscillations due to wave motion have frequencies comparable with turbulent-fluctuation frequencies. Further, propellant residence times in rocket combustors are typically only 3–10 times the mean-turbulent fluctuation periods, therefore, an element of propellant is effected only slightly by turbulence, even during steady-state operation. In addition, gas-phase cross convective flows overwhelm the effects of turbulence.

readily by their appearance in both the gas and spray equations, but with opposite signs). Coupling term expressions and initial and boundary conditions are needed to complete the formulation; they are discussed later under Applications.

Spray-Phase Conservation Equations

a) Droplet number concentration

$$\partial N_j^n/\partial t + \operatorname{div}(\mathbf{u}_j^n N_j^n) = 0 \tag{1}$$

b) Droplet-spray mass density

$$\partial \rho_j^n/\partial t + \operatorname{div}(\mathbf{u}_j^n \rho_j^n) = -N_j^n \dot{m}_{j_{\text{vap}}}{}^n - N_j^n \dot{m}_{j\text{BU}}{}^n - \text{any other mass-loss mechanism} \tag{2}$$

The individual droplet mass may be related to the droplet diameter by relationships involving radial temperature and density gradients in the droplet or as simply as

$$m_j^n = (\pi/6)(D_j^n)^3 \rho_{l,j}{}^n \tag{3}$$

if the drop temperature is uniform. Note: $\rho_j^n = N_j^n m_j^n$ always.

c) Droplet momentum

$$(\partial/\partial t)(\rho_j^n \mathbf{u}_j^n) + \operatorname{div}(\rho_j^n \mathbf{u}_j^n; \mathbf{u}_j^n) = N_j^n \mathbf{F}_j^n - N_j^n(\dot{m}_{j_{\text{vap}}}{}^n + \dot{m}_{j\text{BU}}{}^n + \ldots)\mathbf{u}_j^n \tag{4}$$

d) Droplet thermal energy

$$(\partial/\partial t)(\rho_j^n H_j^n) + \operatorname{div}(\mathbf{u}_j^n \rho_j^n H_j^n) = N_j^n Q_j^n - N_j^n(\dot{m}_{j_{\text{vap}}}{}^n + \dot{m}_{j\text{BU}}{}^n + \ldots)H_{j_s}{}^n \tag{5}$$

Because the heating rate Q_j^n, affects only the sensible enthalpy of the drop (in the absence of decomposition), this equation (assuming $c_{p_j}{}^n$ to be the constant during the increment of heating) can often be simplified with little loss of accuracy to

$$(\partial/\partial t)(\rho_j^n T_j^n) + \operatorname{div}(u_j^n \rho_j^n T_j^n) = N_j^n Q_j^n / c_{p_j}{}^n - N_j^n(\dot{m}_{j_{\text{vap}}}{}^n + \dot{m}_{j\text{BU}}{}^n + \ldots)T_{j_s}{}^n \tag{6}$$

The energy that is transferred to the gas phase is the surface enthalpy so it is still necessary to calculate $H_{j_s}{}^n$. Strictly, In Eqs. (5) or (6), $H_{j_s}{}^n = \mathrm{H}_j{}^n i$ in cases of nonuniform heating, Eq. (5) or (6) is replaced by the droplet thermal-conduction equations and an integral relationship for the total enthalpy throughout the drop.

Gas-Phase Conservation Equations

a) Reduction of species conservation to mixture-ratio conservation

1) Species-conservation equation

$$\partial(\rho\omega_i)/\partial t + \operatorname{div}(\rho\omega_i \mathbf{u}) + \operatorname{div}(\rho\omega_i \mathbf{U}_i) = r_i + \sum_n \sum_j [\Omega_{i,j} N_j^n(\dot{m}_{j_{\text{vap}}}{}^n + \dot{m}_{j\text{BU}}{}^n + \ldots)] \tag{7}$$

Under the assumptions that: 1) the usual binary-diffusion approximation holds

$$\rho\omega_i \mathbf{U}_i = \rho \mathscr{D}_i \operatorname{grad} \omega_i \tag{8}$$

where $\mathscr{D}_i$, the gas-phase diffusion coefficients, are considered to be nearly equal for all species, and 2) gas-phase reaction rates are large compared to the delivery rate of vaporized species from spray droplets to the gas stream, the species conservation equation rigorously reduces to the following relation for the local time varying mixture ratio.

2) Mixture-ratio equation

$$\partial(\rho c)/\partial t + \operatorname{div}(\rho \mathbf{u} c) - \rho\mathscr{D}\{\operatorname{div}(\operatorname{grad} c) - 2|\operatorname{grad} c|^2/c + 1\} - \{\operatorname{grad} c \cdot \operatorname{grad} \rho\mathscr{D}\} = (2c+1)\left\{\sum_n \sum_j^{\text{oxid}} N_j^n(\dot{m}_{j_{\text{vap}}}{}^n + \dot{m}_{j\text{BU}}{}^n + \ldots)\right\} - c^2\left\{\sum_n \sum_j^{\text{fuel}} N_j^n(\dot{m}_{j_{\text{vap}}}{}^n + \dot{m}_{j\text{BU}}{}^n + \ldots)\right\} \tag{9}$$

The mixture-ratio equation is used in conjunction with tables that provide all gas-phase equilibrium properties as functions of c, H, and p for nonsteady-state calculations in which the complete energy equation must be retained, and of c, $H_{o_{inj}}$, and p_o for steady-state calculations in which the complete energy equation may be replaced by a simplified form with a minimum error in gas temperature. In practice, it has been found that effects due to diffusion are masked by gas-phase convective velocities, and hence, $\mathscr{D}$ may be set equal to zero.

b) Global continuity

$$\partial(\rho)/\partial t + \operatorname{div}(\rho \mathbf{u}) = \sum_n \sum_j \left(N_j^n(\dot{m}_{j_{\text{vap}}}{}^n + \dot{m}_{j\text{BU}}{}^n + \ldots)\right) \tag{10}$$

c) Gas momentum

$$\frac{\partial(\rho\mathbf{u})}{\partial t} + \operatorname{div}(\rho\mathbf{u}; \mathbf{u}) = -\operatorname{grad} p + \operatorname{div}\tau - \sum_n \sum_j N_j^n \mathbf{F}_j^n + \sum_n \sum_j N_j^n(\dot{m}_{j_{\text{vap}}}{}^n + \dot{m}_{j\text{BU}}{}^n + \ldots)\mathbf{u}_j^n \tag{11}$$

d) Gas energy

$$\frac{\partial\{\rho(H + u^2/2)\}}{\partial t} + \operatorname{div}\left\{\rho\mathbf{u}\left(H + \frac{u^2}{2}\right)\right\} = -\operatorname{div}\mathbf{q} + \operatorname{div}\mathbf{u}\tau - \sum_n \sum_j N_j^n Q_j^n - \sum_n \sum_j N_j^n \mathbf{u}_j^n \cdot \mathbf{F}_j^n + \sum_n \sum_j N_j^n \times \left\{(\dot{m}_{j_{\text{vap}}}{}^n + \dot{m}_{j\text{BU}}{}^n + \ldots)\left(H_{j_s}{}^n + \frac{(u_j^n)^2}{2}\right)\right\} + \frac{\partial p}{\partial t} \tag{12}$$

e) State

$$\frac{p}{\rho} = R_u T\left[\sum_i \frac{\omega_i}{M_{w_i}}\right]^{-1} \tag{13}$$

The drag vector is given by

$$\mathbf{F}_j^n = \frac{\pi}{8}\{\rho(D_j^n)^2 |\mathbf{u} - \mathbf{u}_j^n|(\mathbf{u} - \mathbf{u}_j^n) C_{D_j}{}^n\} - 24\pi(D_j^n)^3 \operatorname{grad} p$$

The drag force includes both frictional drag and the drag due to volume forces across the drop arising from a pressure gradient. Use of a drag coefficient, $C_{D_j}{}^n$, determined for drops in a steady nearly-constant-pressure flowfield is correct for accelerating drops.

Applications

Application of the comprehensive model requires reduction from vector notation to a coordinate system, imposition of initial and boundary conditions and statement of values for coupling terms. Examples are summarized in this section of reduction to a three-dimensional steady-state combustion model and to a one-dimensional multiple stream-tube combustion model, both in conjunction with analysis of ablative-chamber compatibility.

In reducing the general equations to one spatial dimension, it is necessary to replace ρ, ρ_j^n and N_j^n by $A\rho$, $A\rho_j^n$ and AN_j^n, respectively, when these appear in the left-hand sides of the mass, momentum, and energy-conservation equations. In addition, the entire right-hand sides of these equations must be multiplied by A.

Evaluation of Coupling Terms

Having maintained as complete a model formulation as is practical for computer solution, the accuracy of the solution obtained depends strongly upon the validity of the coupling terms utilized. The three coupling terms usually accounted for are: vaporization rate, $\dot{m}_{j_{\text{vap}}}{}^n$, droplet-heating rate, Q_j^n, and drag force, $\mathbf{F}_j^n$; these are discussed briefly here. The comprehensive model can accommodate droplet-breakup rate, $\dot{m}_{j\text{BU}}{}^n$, and droplet-mass losses from any other conceivable mechanism. Over-all exchange rates are obtained by calculating single droplet behavior, then summing over-all droplets.

Most previous combustion models have used one or the other of two approaches to simultaneously consider droplet heating and evaporation. The quasi-steady evaporation coefficient $[k' = -d(D^2)/dt]$ approach considers the droplet usually to be surrounded by a thin stoichiometric flame zone and the droplet temperature to be constant, i.e., $Q_j^n = 0$ (see Ref. 15). El Wakil's transient droplet-heating approach, detailed in Ref. 7, considers a uniform temperature drop heating and vaporizing in a flowing

gas. The gas temperature is that corresponding to the bulk gas-mixture ratio. No flame zone surrounds the droplet. Rather, the convective flow sweeps the flame off the drop and the vaporized propellant burns beyond the drop in the wake. At the "wet bulb" conditions ($Q_j'' = 0$). this model reduces to the k' approach except the outer boundary condition is the bulk-gas temperature rather than a thin fiim zone. In many circumstances of high-convective flow rates the El Wakil equations appear to give good correlation of predicted and observed behavior. More recent analyses, reviewed by Rosner in Ref. 3, have dealt with flame stability and the distinction between thin flame and purely vaporization exchange mechanisms. In any case, heating and gasification rates are enhanced by forced convection; the empirical Nusselt number correlation of Ranz and Marshall[16] is invariably employed. Burning rates may be enhanced further by vapor phase decomposition and by droplet temperatures approaching the critical temperature; analytical methods for these phenomena are discussed in Refs. 8 and 23. Also, temperature gradients in the liquid may be important in hastening the achievement of high-burning rates.[14,23]

Calculation of the drag force is accomplished primarily through specification of the droplet-drag coefficient. Usually employed are empirical expressions [e.g., Eq. (17), given later] derived from experimental studies of single droplet dynamics. Drag coefficients for droplets deviate substantially from those for solid spheres because of internal circulation, distortion, and vaporization. Rudinger[17] has shown that even small numbers of flowing solid particles apparently have higher effective drag coefficients than do single particles. Similar work has not been accomplished with dense sprays; indeed, drag coefficients have not been determined under any actual rocket conditions. A complete review of existing coupling term expressions and the problems involved in using them to analyze both steady state and transient rocket combustion appears in Ref. 23.

Injector/Chamber Compatibility Analysis¶

The first use of the combustion model given in the previous section was in a general computerized analysis of the effects of injector configuration upon ablative-wall compatibility. For this problem, the general model was specialized to a cylindrical thrust-chamber geometry, steady-state conditions, and sprays formed by impinging liquid stream injectors.

Use of expressions based upon single drops limits the combustion analysis to regions in which the liquid phase can be treated as a field of separated spherical droplets; therefore, the combustion models are applied only downstream of the injection atomization zone of Fig. 1. A separate analysis was developed to describe the distribution of fuel and oxidizer-spray mass, drop sizes, drop velocity vectors, and approximate percentages of liquid vaporized at the boundary between the injection zone and the three-dimensional rapid combustion zone.

A three-dimensional, steady-state model was developed for the rapid combustion zone. It was followed by, and provided input for, a multiple stream tube combustion model applied over the stream-tube zone of Fig. 1.

The combustion models ignore boundary-layer effects at the chamber walls, calculating instead a local "freestream" flow next to the wall. For compatibility calculations, a separate boundary-layer analysis based upon the local freestream flow is, therefore, required to define the heat-transfer coefficients which affect subsequent wall response. Uncoupling the calculation of the combustion flowfield from the wall heat transfer is particularly applicable for ablative chambers because surface temperatures approach the adiabatic-wall temperature and heat-transfer rates are low. The actual local char rates and surface erosion of the ablative walls may then be calculated by any of the available transient conduction/ablation analyses.[18]

When the separate analyses are combined, the over-all analysis is a system of linked calculations which is too unwieldly for a single computer program. The analysis was, therefore, developed into a system of separate computer programs that can be employed individually or in a number of flexible sequences to solve a variety of thrust-chamber design problems. The programs are:

1) LISP (Liquid-Injector Spray Patterns), which calculates bipropellant spray parameters at an array of mesh points (r, θ) in plane Z_o for particular injector configurations.

2) 3-D COMBUST which utilizes the input from LISP and solves for local burning rates, pressure, gas-mixture ratio, velocity vectors, and spray migration from its original distribution by marching from Z_o to the start of the stream-tube zone.

3) STRMTB which calculates continuing spray combustion and acceleration of gases and unburned spray down to the nozzle throat.

4) BLEAT (Boundary-Layer Heat Transfer) calculates local heat-transfer coefficients, adiabatic-wall temperatures, and corrosive-gas composition at the chamber wall based upon local wall-mixture ratios and flow parameters as calculated by 3-D COMBUST and STRMTB.

5) 3-D DEAP and 2-D ABLATE which calculate ablative wall response on either a three-dimensional or an axisymmetric basis.

Details of the boundary layer and wall-response programs, which are outside the scope of this paper, are presented in Ref. 18.

Injector-Spray Analysis, LISP

The LISP computer program calculates spray-mass fluxes (g/cm^2-sec) at mesh points (r, θ, Z_o) by the straightforward summation of the mass fluxes from individual injector elements

$$W(r,\theta,Z_o) = \sum_{i=1}^{N_{EL}} w_i(r,\theta,Z_o) \tag{14}$$

which was first applied by Rupe[19] to analyze the Corporal engine. The method can be used if 1) the individual injector elements have predictable spray-flux patterns which can be measured and correlated; 2) the individual spray patterns of the various elements are not destroyed, between the element impingement points and the plane Z_o, by collisions between neighboring sprays; and 3) vaporization of injected spray mass between the element-impingement points and plane Z_o can be estimated.

These requirements are satisfied when the element orifices have sufficient length/diameter ratio and surface roughness to provide fully developed turbulent-velocity profiles in the impinging liquid streams and when Z_o is on the order of 2 to 5 cm downstream of the impingement points.[20]

The necessary correlation for $w\ (r,\theta,Z_0)$ for use in Eq. (14) is based upon the shape of single element spray-flux distributions determined from cold-flow spray measurements. Rupe's data for unlike doublets, for example, exhibited mass distributions with the general shapes shown in Fig. 2.** Characteristic flux con-

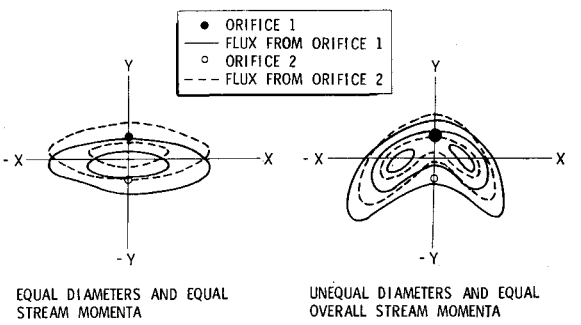

Fig. 2 Characteristic spray flux patterns for the unlike-doublet element.

¶ Research described in this section was performed under Contract FO4611-68-C-0043. This work has been reported in detail in Ref. 18.

** Appreciation is extended to J. Rupe and F. Gerbracht of the Jet Propulsion Laboratory for supplying unpublished cold-flow data from the investigations in Refs. 19 and 21.

tours for triplet and four-on-one elements are described in Refs. 18 and 20. Flux patterns were fitted to the generalized expression

$$w_i(x,y,z) = \frac{w_{001}}{z^2}\left\{\left[1+C_1\left(\frac{y}{z}\right)+C_2\left(\frac{y}{z}\right)^2\right]+\left[C_3\left(\frac{x}{z}\right)+C_4\left(\frac{x}{z}\right)^2\right]\left[1+C_5\left(\frac{y}{z}\right)+C_6\left(\frac{y}{z}\right)^2\right]\right\}\times \exp\left[-a\left(\frac{x}{z}\right)^2-b\left(\frac{y}{z}\right)^2\right] \quad (15)$$

which is applied separately to each propellant from an element. The (x, y, z) coordinate system in Eq. (15) is referenced to the impingement point of the element. The empirical coefficients a, b, w_{001} and C_1 through C_6 are functions of such parameters as element-type (doublet, triplet, etc.) impingement angle, orifice diameter, impinging stream momenta, orifice length, and manifold effects. The form of Eq. (15) was chosen because it satisfies continuity, predicts the observed inverse square relationship between mass flux and distance from the impingement point, and because closed form integrals of Eq. (15) and its x and y moments over the x, y plane allow straightforward evaluation of the empirical coefficients, using experimental cold-flow data.

The LISP computer program transforms the x, y, z coordinate systems of the individual elements to the r, θ, z coordinate system of the thrust chamber and then sums the spray-mass fluxes from the individual injector elements to each point in a uniform matrix of mesh points in plane Z_o. Droplet-velocity vectors are calculated using assumptions that drops travel as straight lines between the impingement point and the mesh points in Z_o and that the propellants' injection velocities are conserved by the drops.

Calculation of mean propellant droplet diameters utilizes empirical equations relating them to injection element hole sizes and injection velocities. Since the equations were derived from cold-flow studies with molten wax jets,[22] corrections accounting for differences in liquid and gas properties between those experiments and the combustor are also applied.

Partial propellant evaporation upstream of Z_o is calculated by a simple evaporation expression

$$w'(r,\theta,Z_o) = w(r,\theta,Z_o)\left[1-(C_{k'}\Delta z/D^2 u_d \rho_l)\right]^{3/2} \quad (16)$$

where w' is the liquid spray flux actually arriving at the point (r, θ, Z_o). Lumped into the coefficient $C_{k'}$ are not only an evaporation coefficient, a Nusselt number, and unit conversions, but also allowance for the fact that the spray is not fully atomized over the entire distance Δz.

Input to the LISP computer program consists of the number, location, orientation, size, geometry, and type of injector elements, together with the geometry of combustion-zone mesh network and general data concerning the propellant densities and injector pressure drops. Up to 50 injector elements can be considered together with as many as 400 combustion zone mesh points.

Rapid Combustion Zone Model, 3-D COMBUST.

The 3-D COMBUST computer program employs three major simplifying assumptions to compute the gas-phase flow-field in the rapid-combustion zone 1) viscous terms in the gaseous momentum equation are small compared to the transverse-convective flow terms; 2) the gas-phase energy equation may be replaced by a table of combustion gas stagnation properties as functions only of mixture ratio; and 3) the term $u_z \partial\rho/\partial z$ is small compared to the other terms in the continuity equation. Except for assumption 3), the continuity equation retains its complete form, the mixture-ratio equation neglects only diffusion terms, and the gas-phase energy equation has been simplified as above. The spray-phase equations include all terms in the r, θ, z coordinate system as presented in the vector-tensor equations except for the transient terms. The sets of liquid and gas governing equations are coupled through mass and momentum exchange between phases. The drag coefficient is specified as

$$C_D = 24\,Re^{-0.84}, \quad Re \leqq 80$$
$$C_D = 0.271\,Re^{0.217}, \quad Re > 80 \quad (17)$$

For droplet gasification, the simple evaporation coefficient model, corresponding to $Q_j^n = 0$, was utilized

$$\dot{m}_j^n = N_j^n(\pi/8)\rho_{l_j}{}^n D_j^n Nu_j^n k_{s_j}{}'^n \quad (18)\dagger\dagger$$

where (Ref. 15)

$$k_{s_j}{}'^n = \frac{8}{\rho_{l_j}{}^n}\int_{T_d}^{T}\frac{k_g}{\Delta H_v + \int_{T_d}^{T} c_{p_v}\,dT}\,dT \quad (19)$$

Other coupling mechanisms are presently neglected. Specification of appropriate boundary conditions, including the initial plane, complete the model.

In principle, a numerical solution of the three-dimensional gas flowfield can be obtained by solving simultaneously the three gas-momentum equations, the state equation, and the mass and mixture-ratio continuity equations for the six unknowns u_z, u_r, u_θ, p, ρ, and c. Even though the energy equation has been eliminated, a number of difficulties exist with this calculation scheme. The greatest problem is that the partial differential equations for the gas phase are of mixed hyperbolic and elliptic type‡‡ and therefore, the analysis is badly posed as an initial value problem. To solve the system of equations as an eigenvalue problem requires a full specification of the unknowns at all r, θ locations of the interface with the following stream-tube zone. But the degree of combustion at this downstream interface is initially unknown, therefore, the spray concentrations and the spray and gas velocities are also unknown; and, in addition, the pressure distribution that backs up into the chamber is also unavailable.

As a consequence, an alternate calculation has been developed for the gas flowfield that permits straightforward marching calculations without numerical instabilities. Because trial calculations indicated that the transverse-pressure gradients must ordinarily remain very small ($\leqq 10^{-4}$ atm/cm) except for the region close to the injector, a simplified prescription for the transverse-pressure gradients was defined as

$$\partial p/\partial r \simeq 0 \qquad \partial p/\partial\theta \simeq 0$$

which becomes equivalent to

$$(\partial p/\partial z)(r,\theta,z) = (\partial p/\partial z)(z \text{ only}) \quad (20)$$

The prescription of uniform transverse-pressure eliminates the elliptic character of the system and permits marching calculations. However, because the simplification introduces errors in transverse gas velocities in proportion to the square roots of the true pressure gradients, the present three-dimensional model must critically be viewed as a calculation that acts to distribute the propellant sprays more realistically than would be the case if they were frozen into a stream-tube structure immediately downstream of the prereaction zone while only approximating the radial and angular-gas velocities.

With assumption 3) stated previously, the differential gas-phase continuity equation becomes

$$\frac{1}{r}\frac{\partial}{\partial r}(ru_r)+\frac{u_r}{\rho}\frac{\partial\rho}{\partial r}+\frac{1}{r}\frac{\partial u_\theta}{\partial\theta}+\frac{u_\theta}{r\rho}\frac{\partial\rho}{\partial\theta}=\frac{\dot{m}}{\rho}-\frac{\partial u_z}{\partial z}=\omega-\frac{\partial u_z}{\partial z} \quad (21)$$

Approximate calculations of gas generation using the droplet-evaporation model for spray distributions close to the injector show that the volumetric gas-generation rate ω (cm^3/cm^3-sec) typically ranges from 5×10^2 to 5×10^4 depending upon the mean-droplet diameter and element spacing. Close to the injector, where the mean-axial gas velocity is on the order of 50 m per second, the high rate of gas generation compared to axial gas

†† In 3-D COMBUST and STRMTB equations, coupling terms $\dot{m}_j^n$, $\mathbf{F}_j^n$, and Q_j^n have been converted from single droplet to a unit volume basis by multiplying them by N_j^n.

‡‡ A critical analysis of the characteristics of the differential equation was performed by R. Van Wyk and is given in Ref. 18.

throughput is expected to cause continuity considerations to dominate momentum considerations. On this basis, a velocity potential for the transverse-velocity field is defined and Eq. (21) becomes

$$\frac{\partial^2\phi}{\partial r^2}+\frac{1}{r}\frac{\partial\phi}{\partial r}+\frac{1}{\rho}\frac{\partial\phi}{\partial r}\frac{\partial\rho}{\partial r}+\frac{1}{r^2}\frac{\partial^2\phi}{\partial\theta^2}+\frac{1}{r^2\rho}\frac{\partial\phi}{\partial\theta}\frac{\partial\rho}{\partial\theta}=\omega-\frac{\partial u_z}{\partial z}=\omega' \qquad (22)$$

where

$$\partial\phi/\partial r = u_r, \quad (1/r)\,\partial\phi/\partial\theta = u_\theta$$

Definition of a velocity potential implies that the transverse flow is irrotational, an assumption that would ordinarily be considered objectionable in a flow subject to two-phase drag and differing local accelerations and gas production. However, it should be noted that when the drag terms and other viscous effects are not specified a priori, then definition of a velocity potential simply leads to the irrotational flowfield of a planar network of gas sources defined by the local burning rates and sinks defined by the axial acceleration. Therefore, a potential solution can be considered a real (if not accurate) solution as long as viscous effects are outweighed by continuity considerations.

To avoid a simultaneous solution of Eq. (22) and the axial-gas momentum relation for all three gas-velocity components, a final simplification was made based upon the assumption expressed in Eq. (20). The axial-gas velocity was assumed to be essentially uniform at any axial location and was therefore calculated from

$$d[\bar{u}_z(z)]/dz = \int_A \dot{m}(r,\theta,z)\,dA \Big/ \int_A \rho(r,\theta,z)\,dA \qquad (23)$$

Current ability to specify the spray drop size, mass distributions, and initial vaporization at the beginning of the rapid-combustion region do not presently warrant more complicated calculations. The primary purpose of the 3-D COMBUST program is to define the adjustment of the gas and spray flowfields and the degree of combustion across the rapid-combustion zone, and for design purposes these calculations do not require precise definition of gas velocity in this region if the droplet-conservation equations are retained in full rigor.

The computerized numerical solution of the entire system of partial differential equations for both spray and gas phases involves marching in the z direction from the initial values prescribed at plane Z_o by the LISP computer program. At each subsequent z plane, a simultaneous solution for all variables at all of the r, θ mesh points is accomplished by a predictor-corrector scheme. An alternating direction finite-difference approach is used for most of the equations, employing central differences in the r and θ directions. In the predictor cycle, the linear finite-difference analogs of these equations are implicit in the r direction and explicit in the θ direction. Separate subprograms solve each of the finite-difference equations as well as calculate the coupling terms and gas physical properties as functions of mixture ratio. Use of separate routines gives maximum flexibility for incorporating changes in the models for the various physical processes as warranted by experimental data. Because of practical limitation on digital computer memory and computation time, the 3-D COMBUST program has been structured for a maximum of 15 circumferential and 7 radial-mesh lines and a maximum of 12 drop-size groups.

Stream-Tube Combustion Model, STRMTB

The STRMTB computer program used in the stream-tube combustion zone is based on reduction of the comprehensive model to one dimension and steady state. To be consistent with the preceding 3-D COMBUST program, gas-phase viscous terms are neglected, the gas-phase energy equation is replaced by tables of equilibrium-stagnation properties, and the coupling terms are calculated using Eqs. (17–19). The model is in reality a multiplicity of one-dimensional models, i.e., there is a complete one-dimensional model for each stream tube. As implied by the name "stream tubes," propellant flows (both sprays and combustion gases) which initially enter a stream tube are, thereafter, constrained to flow in that tube; no provisions are made for exchange of mass, momentum, or energy among neighboring stream tubes.

To illustrate the reduction to one dimension, the gas-phase equations for the sth stream tube are

Continuity,

$$\frac{d}{dz}(\rho_s u_s A_s) = A_s \sum_{n,j} (\dot{m}_j^n)_s \qquad (24)$$

Momentum,

$$\frac{d}{dz}(\rho_s u_s^2 A_s) = A_s\left[-g_c\left(\frac{dp}{dz}+\sum_{j,n}(F_j^n)_s\right)+\sum_{j,n}(\dot{m}_j^n)_s(u_{dj}^n)_s\right] \qquad (25)$$

Adiabatic-energy equation,

$$T_s = T_{os}[1-(\gamma_s-1)/2(u_s/a_{os})^2] \qquad (26)$$

where

$$T_{os} = T_o(c_s), \quad \gamma_s = \gamma(c_s), \quad \text{and} \quad M_{ws} = M_w(c_s)$$

are tabulated and

$$a_{os} = (\gamma_s R_u T_{os} g_c/M_{ws})^{1/2}$$

The three-dimensional mixture-ratio distribution equation is replaced simply by integrating the evaporation rates to get gasified flow rates

$$\dot{w}_{js}(z) = \dot{w}_{js}(Z_o)+\int_{z'=Z_o}^{z}\sum_n (\dot{m}_j^n)_s\,dz' \qquad (27)$$

Mixture ratio,

$$c_s = \dot{w}_{\text{oxid},s}(z)/\dot{w}_{\text{fuel},s}(z) \qquad (28)$$

State,

$$\rho_s = pM_{ws}/R_u T_s \qquad (29)$$

In this formulation, $A(z)$ appears as a dependent variable for which a solution must be found. Individual stream-tube areas can vary; however, only under the constraint that the sum over-all stream tubes must equal the local chamber cross-sectional area. This constraint couples the stream tube solutions together. A second constraint (assumed in order to close the problem) is that pressure is constant across any z plane cross section.

The spray phase equations are

Mass continuity,

$$(d/dz)[(\rho_{dj}^n)_s(u_{dj}^n)_s A_s] = -A_s(\dot{m}_j^n)_s \qquad (30)$$

Drop-number continuity,

$$(d/dz)[(N_{dj}^n)_s(u_{dj}^n)_s A_s] = 0 \qquad (31)$$

or, equivalently,

$$(\dot{N}_{dj}^n)_s = (N_{dj}^n)_s(u_{dj}^n)_s A_s = \text{constant}$$

Momentum,

$$(d/dz)[(\rho_{dj}^n)_s(u_{dj}^n)_s^2 A_s] = A_s[g_c(F_j^n)_s-(\dot{m}_j^n)_s(u_{dj}^n)_s] \qquad (32)$$

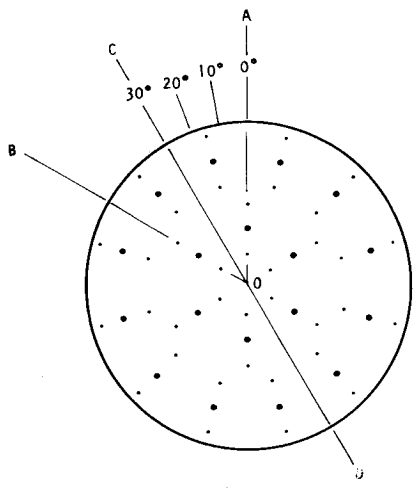

Fig. 3 Eighteen-element triplet injector face pattern.

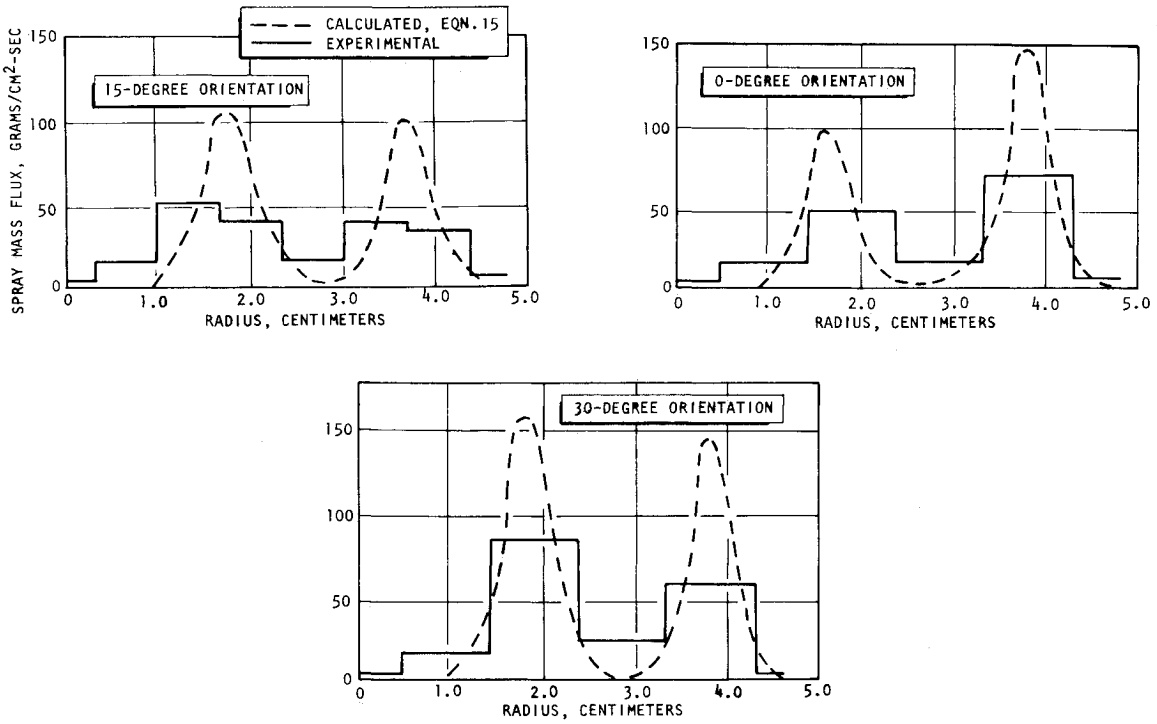

Fig. 4 Experimental vs calculated spray mass flux profiles, triplet injector.

Initial plane conditions are easily derived from the data that have been computed by the 3-D COMBUST program at each r, θ node; appropriate averaging and summing are used if several nodes are combined into one stream tube. Definition of an average initial plane pressure and specification of the cross-sectional area associated with each stream tube are required. Use of punched-card output from the 3-D COMBUST program reduces the labor involved in model interfacing. Alternately, program options permit stream-tube input data to be derived from other sources and the initial plane to be defined at any arbitrary distance downstream of the injector.

The stream-tube model, like any rocket-combustion model, must satisfy a downstream boundary condition in the form of a sonic surface in the neighborhood of the nozzle throat. In the present STRMTB computer program, this is only approximately satisfied in a manner which does not compromise the accuracy of the wall thermal-response analysis. For performance analysis, an improved method has been developed, in which accounting is made of different stream-path lengths and radial-pressure gradients in the nozzle.[24]

Sample Predictions from the Combined Models

A typical system for analysis is illustrated by the 18-element triplet injector shown in Fig. 3. Examination of Fig. 3 shows that the injector consists of repeating sets of the triplet element pattern contained between the rays *OA* and *OB*. In addition, the line *DOC* represents a plane of symmetry. The rays *OA* and *OC*, therefore, define boundaries of symmetry throughout the chamber and nozzle across which there should be no gradients or net flows; consequently, only the thrust-chamber slice between these rays needs to be considered for a complete solution of the combustor flow, temperature, and concentration fields. The computerized analysis was structured to take maximum advantage of planes of symmetry to economize in several areas. Radial baffles, provided they are not too short, also furnish no-flux boundaries equivalent to radial planes of symmetry.

LISP computer-program outputs of spray mass and mixture-ratio distributions for a number of simple doublet and triplet injectors have been evaluated by comparing them with cold-flow experiments using water and trichloroethylene to simulate Aerozine-50 fuel and N_2O_4 oxidizer. The apparatus consisted of a 29×29 matrix of 0.67 cm^2 sampling elements. The predicted spray-mass distribution at a distance of 3.8 cm from the face of the 18-element triplet injector of Fig. 3 is compared in Fig. 4 to a measured distribution corresponding to an over-all mixture ratio of 1.6. Comprisons of mass flux are made along radii corresponding to the 0°, 15°, and 30° angular locations within the repeating segment of the injector, which is typical of the injector as a whole. Qualitative agreement between analytical and experimental results is evident in Fig. 4; quantitative agreement is limited by the resolution of the cold-flow collection apparatus (the histograms of the experimental data represent the average flux for the 0.67 cm^2 individual sampling elements) but is considered to be satisfactory for combustion and chamber-wall response analyses.

Similar satisfactory agreement between analytical predictions and cold-flow experimental data was obtained for a 72-element like-doublet injector and an 8-element unlike-doublet injector[18] when the liquids were collected between 3.5 and 4 cm downstream of the injector face as illustrated in Fig. 5. However, a limited number of experiments with collection at 7–8 cm from the injector indicated that collisions between droplets from different injector elements can contribute to turning of the sprays from a multielement injector. The effect of such collisions is analytically accounted for in the case of droplets belonging to the same propellant and size group by the present system of spray-momentum equations but is ignored for droplets from different groups. Therefore, use of the LISP computer program is currently restricted to the region extending approximately 5 cm from the injector.

The primary objective of the first use of the combustion model was to describe the three-dimensional, two-phase, combustion-chamber flowfield in a manner permitting analysis of the complicated heat transfer in this region. The flow parameters near the wall which are important to local heat transfer include the axial-gas velocity, the radial-gas velocity, and the amount of spray which impinges upon and then evaporates as it flows along the wall. Typical trends for these parameters, as calculated for the triplet injector of Fig. 3, are shown in Fig. 6. The radial-velocity component has become small enough at approximately 7–8 cm from the injector to initiate a stream-tube analysis of the

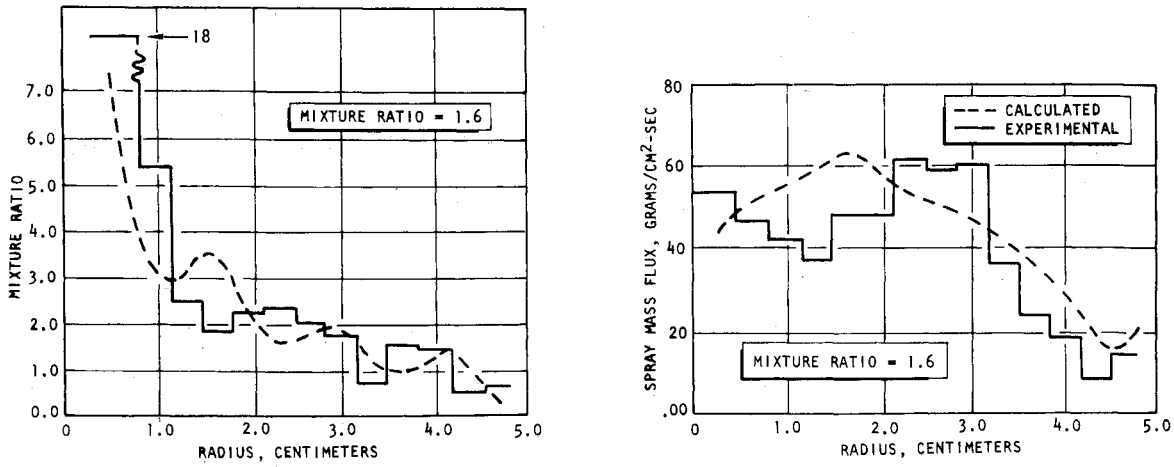

Fig. 5 Spray mass and mixture-ratio distributions, like-doublet injector.

flowfield. Also, at that point, heat-transfer analysis based upon an essentially one-dimensional main gas stream can be initiated. Figure 6 shows that spray evaporation along the chamber walls can persist for significant distances, thereby, contributing to low-net heat-transfer rates. The heat-transfer analysis based on data computed by the combustion models is contained within the BLEAT boundary-layer computer program described in Ref. 18. The predicted axial heat-flux distributions corresponding to the 332° and 17° angular locations of the triplet injector of Fig. 3 are compared to experimental data in Fig. 7. The agreement is excellent, particularly in the delineation of a region of minimum heat transfer about 7–8 cm from the injector corresponding almost simultaneously to the disappearance of radial-combustion field velocities and the maximum rate of spray evaporation along the walls.

References

[1] Lewis, J. D., "Studies of Atomization and Injection in the Liquid Propellant Rocket Engine," *Combustion and Propulsion, Fifth AGARD Colloquium: High-Temperature Phenomena*, Macmillan, New York, 1963, pp. 141–169.

[2] Lambiris, S., Combs, L. P., and Levine, R. S., "Stable Combustion Processes in Liquid Propellant Rocket Engines," *Combustion and Propulsion, Fifth AGARD Colloquium: High-Temperature Phenomena*, Macmillan, New York, 1963, pp. 569–634.

[3] Harrje, D. T. and Reardon, F. H., *ICRPG Reference Book on Liquid-Rocket Combustion Instability*, Princeton Univ., Princeton, New Jersey (in press, 1971).

[4] Bittker, D. A. and Brokaw, R. S., "Estimate of Chemical Space Heating Rates in Gas-Phase Combustion, With Application to Rocket Propellants," *ARS Journal*, Vol. 30, No. 2, Feb. 1960, p. 179.

[5] Williams, F. A., *Combustion Theory*, Addison-Wesley, Reading, Mass., 1965, Chap. 11.

[6] Spalding, D. B., "A One-Dimensional Theory of Liquid Fuel Rocket Combustion," TR 20-175, 1959, Aeronautical Research Council, London.

[7] Priem, R. J. and Heidmann, M. F., "Propellant Vaporization as a Design Criterion for Rocket Engine Combustion Chambers," TR R-67, 1960, NASA.

[8] Campbell, D. T. and Chadwick, W. D., "Combustion Instability Analysis at High Chamber Pressures," AFRPL-TR-68-179, Aug. 1968, Rocketdyne, North American Rockwell Corp., Canoga Park, Calif.

[9] Crocco, L. and Cheng, S. I., *Theory of Combustion Instability in Liquid Propellant Rocket Motors*, AGARDograph No. 8, 1956, Butterworths, London.

[10] Crocco, L., "Theoretical Studies on Liquid Propellant Rocket Instability," *Tenth Symposium (International) on Combustion*, The Combustion Inst., Pittsburgh, Pa., 1965, pp. 1101–1128.

[11] Burstein, S. Z. and Agosta, V. D., "Combustion Instability: Non-Linear Analysis of Wave Propagation in a Liquid Propellant Rocket Motor," AFOSR TN-2619, March 1962, Polytechnic Inst. of Brooklyn, New York.

[12] Priem, R. J. and Guentert, D. C., "Combustion Instability Limits Determined by a Non-Linear Theory and a One-Dimensional Model," TN D-1409, Oct. 1962, NASA.

[13] Burstein, S. Z. and Schechter, H., "A Two-Dimensional Time-

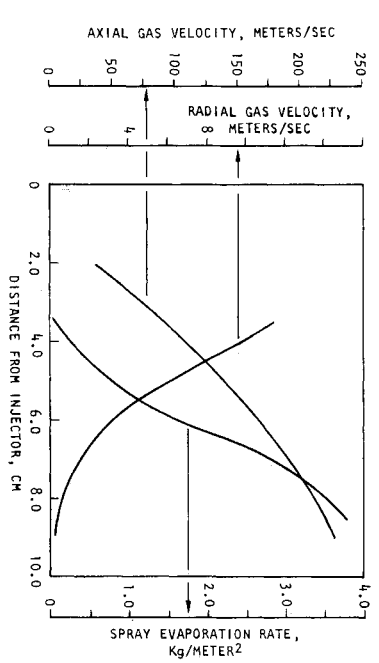

Fig. 6 Variation of combustion parameters with distance from the injector for the 18-element triplet of Fig. 3.

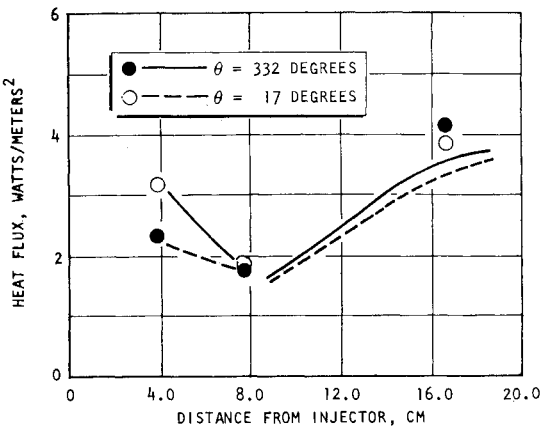

Fig. 7 Comparison of calculated and experimental heat fluxes for the triplet injector of Fig. 3.

Dependent Annular Combustion Model," *6th ICRPG Combustion Conference, CPIA Publication 192,* Dec. 1969, Chemical Propulsion Information Agency, Silver Spring, Md.

[14] Agosta, V. D., "Nonlinear Combustion Instability: Longitudinal Mode," *6th ICRPG Combustion Conference, CPIA Publication 192,* Dec. 1969, Chemical Propulsion Information Agency, Silver Spring, Md.

[15] Penner, S. S., *Chemistry Problems in Jet Propulsion,* Pergamon Press, New York, 1960.

[16] Ranz, W. E. and Marshall, W. R. Jr., "Evaporation From Drops," *Chemical Engineering Progress,* Vol. 48, No. 3, 1952, pp. 141–146; also Vol. 48, No. 4, 1952, pp. 173–180.

[17] Rudinger, G., "Effective Drag Coefficients for Gas-Particle Flow in Shock Tubes," *Transactions of the ASME; Journal of Basic Engineering,* Vol. 92, Ser. D, No. 1, March 1970, pp. 165–172.

[18] Hines, W. S., Combs, L. P., Ford, W. M., and Van Wyk, R., "Development of Injector Chamber Compatibility Analysis," AFRPL-TR-70-12, March 1970, Rocketdyne, North American Rockwell Corp., Canoga Park, Calif.

[19] Rupe, J. H. and Jaivin, G. H., "The Effects of Injection Mass Flux Distributions and Resonant Combustion on Local Heat Transfer in a Liquid-Propellant Rocket Engine," Progress Rept. 32-648, Oct. 1964, Jet Propulsion Lab., Pasadena, Calif.

[20] Hines, W. S., Hyde, J. C., Chadwick, W. D., and Ford, W. M., "Analytical Description of Injected Propellant Spray Mass Distributions," *6th ICRPG Combustion Conference, CPIA Publication 192,* Dec. 1969, Silver Spring, Md.

[21] Rupe, J. H., "The Liquid-Phase Mixing of a Pair of Impinging Streams," Progress Rept. 20-195, Aug. 1953, Jet Propulsion Lab., Pasadena, Calif.

[22] Dickerson, R. A., Tate, K., and Barsic, N., "Correlation of Spray Injector Parameters With Rocket Engine Performance," AFRPL-TR-68-147, June 1968, Rocketdyne, North American Rockwell Corp., Canoga Park, Calif.

[23] Sutton, R. D., "Propellant Spray Combustion Processes During Stable and Unstable Liquid Rocket Combustion," AFOSR TR-2714, Oct. 1970, Rocketdyne, North American Rockwell Corp., Canoga Park, Calif.

[24] Combs, L. P., Chadwick, W. D., and Campbell, D. T., "Liquid Rocket Performance Computer Model With Distributed Energy Release, Interim Final Report," R-8298, Sept. 1970, Rocketdyne, North American Rockwell Corp., Canoga Park, Calif.